

Bond-Mediated Electron Tunneling in Ruthenium-Modified High-Potential Iron–Sulfur Protein

Elena Babini,^{1a} Ivano Bertini,^{1b} Marco Borsari,^{1c}
 Francesco Capozzi,^{1d} Claudio Luchinat,^{*,1e} Xiaoyu Zhang,^{1f}
 Gustavo L. C. Moura,^{1f} Igor V. Kurnikov,^{1f}
 David N. Beratan,^{*,1f} Adrian Ponce,^{1g} Angel J. Di Bilio,^{1g}
 Jay R. Winkler,^{*,1g} and Harry B. Gray^{*,1g}

Departments of Chemistry, University of Florence
 via Gino Capponi, 50121 Florence, Italy
 University of Modena, via Campi 183
 41100 Modena, Italy
 University of Calabria
 87036 Arcavacata di Rende (CS), Italy
 University of Pittsburgh, Pittsburgh, Pennsylvania 15260
 Institute of Agricultural Chemistry, University of Bologna
 viale Berti Pichat 10, 40127 Bologna, Italy
 Department of Soil Science and Plant Nutrition
 University of Florence, P.le delle Cascine 28
 50144 Florence, Italy
 Beckman Institute, California Institute of Technology
 Pasadena, California 91125

Received December 22, 1999

High-potential iron–sulfur proteins (HiPIPs)² are found in photosynthetic purple nonsulfur bacteria.³ The three-dimensional structure of *Chromatium vinosum* HiPIP features two short segments of α -helix, three strands of antiparallel β -pleated sheet, and a small helix near the N-terminus.⁴ The cubane $[\text{Fe}_4\text{S}_4]$ cluster is attached covalently to the polypeptide matrix through Fe–S⁺ bonds to cysteines 43, 46, 63, and 77. The side chains of Tyr19, Phe48, Trp60, Phe66, Trp76, Trp80, and other nonpolar residues encapsulate the cluster in a hydrophobic cavity that is inaccessible to solvent.⁵ Tyr19, which contacts the $[\text{Fe}_4\text{S}_4]$ core, has been suggested to play a particularly important structural role.⁶ In both oxidation states, the cysteinyl and core inorganic sulfur atoms are involved in H-bonding interactions with peptide NH protons.⁷

We have studied intramolecular electron transfer in *C. v.* HiPIPs in which surface histidines at positions 18, 42, 50, and 81 (42 is wild type; 18, 50, and 81 are mutants in which 42 is Gln)⁸ were modified by coordination of Ru(bpy)₂(im)²⁺ (Figure 1A).^{9,10} The calculated $[\text{Fe}_4\text{S}_4]^{2+}$:[Ru(HisX)]³⁺ electronic couplings in these four Ru-modified proteins vary dramatically, even though the closest Fe–Ru ET distances fall in a narrow range (Figure 1B–

(1) (a) University of Bologna. (b) University of Florence, 50121 Florence. (c) University of Modena. (d) University of Calabria. (e) University of Florence, 50144 Florence (e-mail, luchinat@cerm.unifi.it). (f) University of Pittsburgh (e-mail, beratan@pitt.edu). (g) California Institute of Technology (e-mail, hgcm@its.caltech.edu; winklerj@its.caltech.edu).

(2) Abbreviations: HiPIP, high-potential iron–sulfur protein; *C. v.*, *Chromatium vinosum*; ET, electron transfer; bpy, 2,2'-bipyridine; dmbyp, 4,4'-(CH₂)₂2,2'-bipyridine; im, imidazole; NHE, normal hydrogen electrode; HEPES, *N*-[2-hydroxyethyl]piperazine-*N'*-[2-ethanesulfonic acid]; Pi, phosphate.

(3) Capozzi, F.; Ciurli, S.; Luchinat, C. *Struct. Bonding* **1998**, *90*, 127–159. Cowan, J. A.; Lui, S. M. *Adv. Inorg. Chem.* **1998**, *45*, 313–350. Bonora, P.; Principi, I.; Monti, B.; Ciurli, S.; Zannoni, D.; Hochkoeppler, A. *Biochim. Biophys. Acta* **1999**, *1410*, 51–60. Beinert, H. *JBIC* **2000**, *5*, 2–15.

(4) Parisini, E.; Capozzi, F.; Lubini, P.; Lamzin, V.; Luchinat, C.; Sheldrick, G. M. *Acta Crystallogr.* **1999**, *D55*, 1773–1784. Carter, C. W.; Kraut, J.; Freer, S. T.; Xuong, N.-H.; Alden, R. A.; Bartsch, R. G. *J. Biol. Chem.* **1974**, *249*, 4212–4225.

(5) Soriani, A.; Cowan, J. A. *Inorg. Chim. Acta* **1996**, *251*, 285–290. Bian, S.; Hemann, C. F.; Hille, R.; Cowan, J. A. *Biochemistry* **1996**, *35*, 14544–14552.

(6) Agarwal, A.; Li, D.; Cowan, J. A. *Proc. Natl. Acad. Sci. U.S.A.* **1995**, *92*, 9440–9444.

(7) Backes, G.; Mino, Y.; Loehr, T. M.; Meyer, T. E.; Cusanovich, M. A.; Sweeney, W. V.; Adman, E. T.; Sanders-Loehr, J. *J. Am. Chem. Soc.* **1991**, *113*, 2055–2064.

E). Thus these Ru-HiPIPs provide a particularly rigorous test of the tunneling-pathway model of ET in proteins.^{11,12}

Kinetics of ET from $[\text{Fe}_4\text{S}_4]^{2+}$ to Ru(HisX)³⁺ ($X = 18, 42, 50, 81$) were measured by transient absorption changes following intramolecular quenching of electronically excited Ru-HiPIPs.¹³ Rate constants (k_{ET}) and driving forces ($-\Delta G^\circ$) are set out in Table 1. It is likely that the reorganization energy (λ) is below 1 eV for these reactions, since NMR work has established that the solution structures of oxidized and reduced *C. v.* HiPIP¹⁴ are similar.¹⁵ A value in the 0.6–0.9 eV range^{16–18} accounts for the very small changes in rate that accompany driving-force ($X = 42, 81$) and temperature ($X = 50$)¹⁹ variations. Thus the observed rates closely approximate coupling-limited k_{ET} values.

(8) Recombinant *C. v.* HiPIP was expressed in *E. coli* transformed with the plasmid pEBCV10 containing a synthetic gene encoding for this protein (Babini, E.; Bertini, I.; Borsari, M.; Capozzi, F.; Dikiy, A.; Eltis, L. D.; Luchinat, C. *J. Am. Chem. Soc.* **1996**, *118*, 75–80). The various HiPIPs, namely, (Lys18His, His42Gln), (Gln50His, His42Gln), and (Thr81His, His42Gln), were obtained by site-directed mutagenesis (Kunkel, T. A.; Roberts, J. D.; Zakour, R. D. *Methods Enzymol.* **1987**, *154*, 267–382). (HiPIPs with His residues at $X = 20, 48, 66$ and 78 were expressed as well.) Mutagenesis was carried out on a wild-type uracil-containing single-stranded template to replace His42, and subsequently on the His42Gln template to introduce the second mutation. HiPIPs were extracted and purified as described previously (Eltis, L. D.; Iwagami, S. G.; Smith, M. *Protein Eng.* **1994**, *7*, 1145–1150).

(9) Ruthenium-modified HiPIPs were prepared by reacting reduced protein (~0.1 mM) dissolved in 250 mM NaHCO₃/10 mM HEPES (pH 7.7–8.2) with a 3–5-fold excess of [Ru(bpy)₂CO₃]⁴H₂O (in the case of (His18)HiPIP a 1:1 protein–Ru ratio was used). Details of purification and characterization are given in the Supporting Information. (NH₃)₂Ru(His42)HiPIP (*C. v.*) has been prepared previously (Jackman, M. P.; Lim, M.-C.; Sykes, A. G.; Salmon, G. A. *J. Chem. Soc., Dalton Trans.* **1988**, 2843–2850. Govindaraju, K.; Moulis, J.-M.; Salmon, G. A.; Sykes, A. G. *J. Chem. Soc., Dalton Trans.* **1993**, 643–647).

(10) Di Bilio, A. J.; Dennison, C.; Gray, H. B.; Ramirez, B. E.; Sykes, A. G. *J. Am. Chem. Soc.* **1998**, *120*, 7551–7556.

(11) Beratan, D. N.; Onuchic, J.; Betts, J. N. *Science* **1991**, *252*, 2285–2288. Beratan, D. N.; Onuchic, J.; Winkler, J. R.; Gray, H. B. *Annu. Rev. Biophys. Biomol. Struct.* **1992**, *21*, 349–377. Beratan, D. N.; Skourtis, S. S. *Curr. Opin. Chem. Biol.* **1998**, *2*, 235–243. Regan, J. J.; Onuchic, J. *Adv. Chem. Phys.* **1999**, *107*, 497–553. Skourtis, S. S.; Beratan, D. N. *Adv. Chem. Phys.* **1999**, *107*, 377–452.

(12) Wuttke, D. S.; Bjerrum, M. J.; Winkler, J. R.; Gray, H. B. *Science* **1992**, *256*, 1007–1009. Langen, R.; Chang, I.-J.; Germanas, J. P.; Richards, J. H.; Winkler, J. R.; Gray, H. B. *Science* **1995**, *268*, 1733–1735. Bjerrum, M. J.; Casimiro, D. R.; Chang, I.-J.; Di Bilio, A. J.; Gray, H. B.; Hill, M. G.; Langen, R.; Mines, G. A.; Skov, L. S.; Winkler, J. R.; Wuttke, D. S. *J. Bioenerg. Biomembr.* **1995**, *27*, 295–302. Regan, J. R.; Di Bilio, A. J.; Langen, R.; Skov, L. K.; Winkler, J. R.; Gray, H. B. *Chem. Biol.* **1995**, *2*, 489–496. Gray, H. B.; Winkler, J. R. *Annu. Rev. Biochem.* **1996**, *65*, 537–561. Winkler, J. R.; Gray, H. B. *JBIC* **1997**, *2*, 399–400. Winkler, J. R.; Di Bilio, A. J.; Farrow, N. A.; Richards, J. H.; Gray, H. B. *Pure Appl. Chem.* **1999**, in press.

(13) Excitation of Ru(HisX)²⁺-HiPIP_{ox} gives ^{*}Ru(HisX)²⁺-HiPIP_{ox} intramolecular oxidative quenching yields Ru(HisX)³⁺-HiPIP_{red}, which undergoes $[\text{Fe}_4\text{S}_4]^{2+} \rightarrow \text{Ru}(\text{HisX})^{3+}$ ET. Samples for transient absorption spectroscopy contained 20–30 μM Ru-HiPIP($[\text{Fe}_4\text{S}_4]^{3+}$) (oxidation was achieved by reacting the proteins with excess $[\text{Fe}(\text{CN})_6]^{4-}$ for 3–4 min followed by gel filtration) in pH 7.0 Na or KP_i, and were kept under argon. The apparatus for nanosecond transient absorption has been described previously (Low, D. W.; Winkler, J. R.; Gray, H. B. *J. Am. Chem. Soc.* **1996**, *118*, 117–120; ref 10). ET could be monitored at any wavelength in the range 300–600 nm: $\Delta\epsilon(\text{red-OX})_{\text{HiPIP}} \sim -10800 \text{ M}^{-1} \text{ cm}^{-1}$ (478 nm) (Bartsch, R. G. *Methods Enzymol.* **1971**, *23*, 644–649); $\Delta\epsilon(\text{ox-red})_{\text{Ru}} \sim -7000 \text{ M}^{-1} \text{ cm}^{-1}$ (492 nm), and $\Delta\epsilon(\text{ox-red})_{\text{Ru}} \sim 17500 \text{ M}^{-1} \text{ cm}^{-1}$ (316 nm). A picosecond transient absorption spectrometer (Bachrach, M. Ph.D. Thesis, California Institute of Technology, 1996) was used to measure rates greater than $\sim 2 \times 10^7 \text{ s}^{-1}$ (experimental conditions: $\sim 100 \mu\text{M}$ Ru-protein; λ_{ex} 355 nm, 1 mJ, 10 ps fwhm; λ_{obs} 532 nm; net Ru-HiPIP photoreduction was observed when 355 nm excitation was employed.

(14) Banci, L.; Bertini, I.; Dikiy, A.; Kastrau, D. H. W.; Luchinat, C.; Sompornpisut, P. *Biochemistry* **1995**, *34*, 206–219. Bertini, I.; Dikiy, A.; Kastrau, D. H. W.; Luchinat, C.; Sompornpisut, P. *Biochemistry* **1995**, *34*, 9851–9858. Bertini, I.; Ciurli, S.; Luchinat, C. *Struct. Bonding* **1995**, *83*, 1–53.

(15) The solution structure is very similar to the crystal structure.⁴ There is an average increase of $\sim 0.1 \text{ \AA}$ in the Fe–S distances upon reduction of crystalline material (Carter, C. W.; Kraut, J.; Freer, S. T.; Alden, R. A. *J. Biol. Chem.* **1974**, *249*, 6339–6346).

(16) Values in this range have been obtained from analyses of $-\Delta G^\circ$ and temperature dependences of ET rates in Ru(bpy)₂(im)(His33)cytochrome c (0.74 eV)¹⁷ and Ru(bpy)₂(im)(His33)azurin (0.7 eV).¹⁸

(17) Mines, G. A.; Bjerrum, M. J.; Hill, M. G.; Casimiro, D. R.; Chang, I.-J.; Winkler, J. R.; Gray, H. B. *J. Am. Chem. Soc.* **1996**, *118*, 1961–1965.

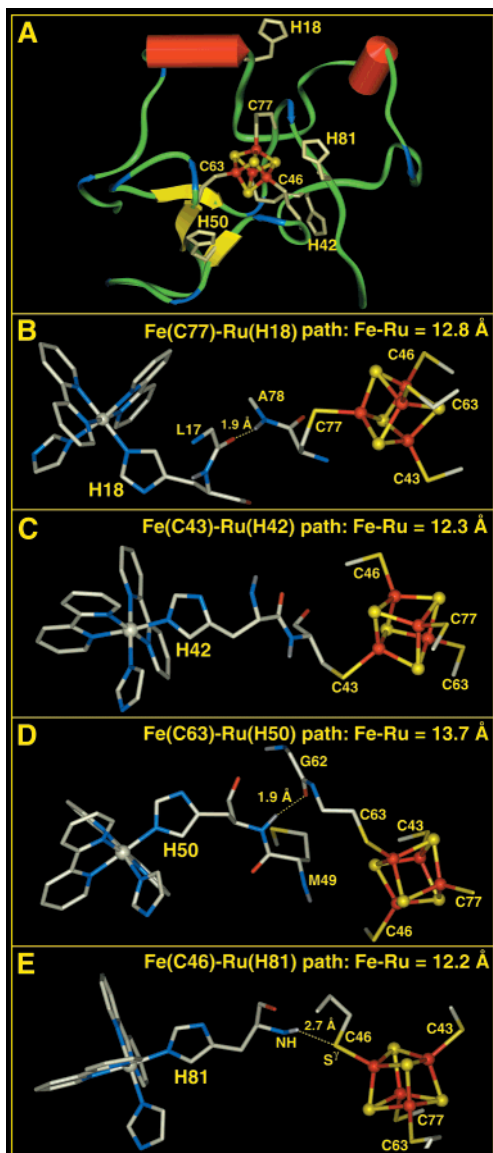


Figure 1. (A) Structure of *C. v.* HiPIP with histidines at positions 18, 42, 50, and 81. (B–E), Electron tunneling pathways in Ru(HisX)-HiPIPs ($X = 18, 42, 50, 81$). Structures were built using HyperChem 5.0 (HyperChem(TM), Hypercube, Inc.: 1115 NW 4th Street, Gainesville, FL 32601) and partially energy minimized using AMBER 4.1 (Pearlman, D. A.; Case, D. A.; Caldwell, J. W.; Ross, W. S.; Cheatham, T. E., III; Ferguson, D. M.; Seibel, G. L.; Singh, U. C.; Weiner, P. K.; Kollman, P. A. *AMBER 4.1*, University of California, San Francisco, 1995.). Atomic coordinates for HiPIP (PDB code 1CKU)⁴ and [Ru(bpy)₂(im)]₂SO₄·10H₂O (Faham, S.; Day, M. W.; Connick, W. B.; Crane, B. R.; Di Bilio, A. J.; Schaefer, W. P.; Rees, D. C.; Gray, H. B. *Acta Crystallogr.* **1999**, *D55*, 379–385; PDB code 1BEX) were used for modeling. Stereochemical and van der Waals constraints place an upper limit of about 1 Å on the uncertainty in Fe–Ru distances.

It is striking that the tunneling times vary over 2 orders of magnitude in proteins in which the distances between Ru and

(18) Di Bilio, A. J.; Hill, M. G.; Bonander, N.; Karlsson, B. G.; Villahermosa, R. M.; Malmström, B. G.; Winkler, J. R.; Gray, H. B. *J. Am. Chem. Soc.* **1997**, *119*, 9921–9922. Skov, L. K.; Pascher, T.; Winkler, J. R.; Gray, H. B. *J. Am. Chem. Soc.* **1998**, *120*, 1102–1103.

Table 1. $[Fe_4S_4]^{2+} \rightarrow Ru(HisX)^{3+}$ ET Data for Ru-HiPIPs^a

protein	k_{ET} (s ⁻¹)	$-\Delta G^\circ$ (eV)
Ru(bpy) ₂ (im)(His18)HiPIP	$6.0(10) \times 10^7$	0.71
Ru(bpy) ₂ (im)(His42)HiPIP	$2.7(5) \times 10^8$	0.65
Ru(dmbpy) ₂ (im)(His42)HiPIP	$1.9(4) \times 10^8$	0.57
Ru(bpy) ₂ (im)(His50)HiPIP	$1.8(2) \times 10^6$	0.69
Ru(bpy) ₂ (im)(His81)HiPIP	$6.1(10) \times 10^8$	0.69
Ru(dmbpy) ₂ (im)(His81)HiPIP	$5.7(10) \times 10^8$	0.61

^a 0.1 M NaPi, pH 7.0, 22 °C. ^b E° (V vs NHE): Ru(bpy)₂(im)(His42)HiPIP[Fe₄S₄]^{3+/2+} = 0.393; [Ru(bpy)₂(im)(His42)]^{3+/2+}HiPIP = 1.046; (Lys18His, His42Gln)HiPIP[Fe₄S₄]^{3+/2+} = 0.341; (Gln50His, His42Gln)HiPIP[Fe₄S₄]^{3+/2+} = 0.356; (Thr81His, His42Gln)HiPIP[Fe₄S₄]^{3+/2+} = 0.352; [Ru(dmbpy)₂(im)]₂^{3+/2+} = 0.96.¹⁷

the closest Fe in the Fe₄S₄ core differ by less than 2 Å. The 340-fold rate difference His50 ≪ His 81 is attributed to a 5-bond shorter pathway in His 81 (His50, 12 covalent bonds plus 1 H-bond; His81, 7 + 1). Pathway predictions of rate ratios for the full set [1(His50):0.36(His18):28(His42):12(His81)],²⁰ however, are different from experimental values [1:30:150:340]. Inclusion of all chemical groups containing atoms that lie on paths within 50% of the strongest path provides a better description of the protein-mediated coupling. Relative rates based on calculated couplings at the Hartree–Fock 3-21G level are [1:18:45:71],²⁰ in accord with the order observed experimentally.

The dramatic rate differences observed for the Ru(HisX)-HiPIPs arise from the nature of the tunneling pathways. The rapid electron tunneling in Ru(His81)-HiPIP underscores the importance of hydrogen-bond-mediated coupling.²¹ The Fe–Ru coupling in this mutant is comparable in strength to that in Ru(His42)-HiPIP, in which the donor, Fe(Cys43), is directly (42–43) coupled to the acceptor. Approximate quantum chemical analysis that includes secondary pathways, interactions beyond nearest neighbors, and orbital symmetry effects accounts for many of the other observed rate differences. We conclude that the relative strengths of the electronic couplings in HiPIP can be understood only in the context of bond-mediated coupling, which takes the three-dimensional structure of the folded protein into explicit account.

Acknowledgment. We thank Brian Crane for helpful discussions. This research was supported by NIH (DK19038 to H.B.G.; GM48043 to D.N.B.), the Howard Hughes Medical Institute (summer undergraduate research fellowship to X.Z.), and CAPES-Brazil (graduate fellowship to G.L.C.M.).

Supporting Information Available: Ruthenium modification procedure; absorption spectra; electrochemical procedure, voltammograms, and reduction potentials for HiPIP and Ru(His42)HiPIP (Ru^{3+/2+} and Fe^{3+/2+} couples) measured at eight different temperatures; HiPIP and ruthenium difference absorption spectra; transient absorption kinetics traces (PDF). This material is available free of charge via the Internet at <http://pubs.acs.org>.

JA994472T

(19) $k_{ET}[Ru(His50)HiPIP]$ is independent of temperature in the range 4–30 °C.

(20) Pathway values are based on metal-to-metal couplings. Searches performed to the edges of the Ru ligands gave similar results. Donor and acceptor groups in the quantum calculations were represented by hydrogen atoms with binding energies of –5 eV. For details of the methodology see: Kurnikov, I. V.; Beratan, D. N. *J. Chem. Phys.* **1996**, *105*, 9561–9573.

(21) Studies of other Ru-modified proteins^{11,12} and donor–acceptor complexes (de Rege, P. J. F.; Williams, S. A.; Therien, M. J. *Science* **1995**, *269*, 1409–1413; Yang, J.; Seneviratne, D.; Arbatin, G.; Andersson, A. M.; Curtis, J. C. *J. Am. Chem. Soc.* **1997**, *119*, 5329–5336; Kirby, J. P.; Roberts, J. A.; Nocera, D. G. *J. Am. Chem. Soc.* **1997**, *119*, 9230–9236; Williamson, D. A.; Bowler, B. E. *J. Am. Chem. Soc.* **1998**, *120*, 10902–10911) have shown that hydrogen-bond bridges can be very effective in mediating distant couplings.